CHAPTER 3

3.1 Introduction

An aggregate of a few tens atoms that are luminescent, non-toxic in nature, and bridge the gap between a single atom and nanoparticle forms the basis of metal nanoclusters [165]. Due to their ultra-small size (~2 nm) [166], novel physicochemical properties emerge, such as multicolor fluorescence or white light emission, finding its wide application in the area of optoelectronics [93,118], cellular imaging [123], photocatalysis [167], batteries [168], and nanomedicine [87,169]. The multicolor fluorescence or white light emission is unique due to its debatable origin. Some believe surface trap states [170], while others support metal core ligands [16,88,171] as the primary source of the origin. Yet others have demonstrated fluxional states of loosely bound atoms in the nanoclusters as the source of white light [172]. To understand the origin of emission in nanoclusters, several tunable fluorescent noble metal nanoclusters have been synthesized with a large extinction coefficient and used as fluorescent probes [173–175]. Despite tremendous success in this area, effective size control, colloidal stability, and low inertness of nanoclusters remain a challenge that needs to be addressed during their synthesis [17,176].

Since biocompatible white light emitting nanoclusters can unleash high contrast multicolor image acquisition in biological systems. They have been mostly prepared by proper mixing of red (R), green (G), and blue (B) spectrum emitting different nanoclusters together [119,177,178]. These nanoclusters are known to achieve different color emissions by changing the capping ligand. These capping ligands are also known to affect overall stability and fluorescence emission of nanoclusters, further making white light emission from single (material, without mix-match) component are challenging to obtain [179]. Due to the high demand of white light emitting (single component) nanoclusters, few white light

emitting nanoparticles with cytotoxic decomposition products [25,26] were reported using very complex synthetic [125,180,181] methods that are hard to follow. Further, due to their large size [182] and non-biodegradable by-products, organ failure [100,183] resulted. Therefore, to address the problem of stable white light emission in a single system, engendering biodegradable by-products, the synthesis of water-soluble metal nanoclusters was taken up [122].

Magnesium (Mg) is an alkaline earth metal and is abundantly found inside our body as an essential metabolite or catalyst for metabolic reactions [77,184,185]. Its decomposition into Mg^{2+} ion is wholly absorbed within [3] the body and doesn't cause additional cytotoxicity and accumulation problems. These biological features make metallic magnesium a critical material for developing nanoclusters with a broader view of bioimaging. Besides, magnesium's rapid electron transfer capability can potentially tune the fluorescence properties of synthesized clusters. It may ultimately generate white light when stabilized with an appropriate capping agent. Besides, white light-emitting Mg^0 nanoclusters have never been reported to the best of our knowledge.

There have been only a few attempts for aqueous phase synthesis of stable magnesium (Mg) nanoclusters, primarily due to its small reduction potential (E° = -2.37 V), low molecular weight (M.Wt. = 24), low density (1.73 g/cm3) [186] and propensity to make oxides [3] etc. Generally, the aqueous phase stability of nanoclusters and their multicolor fluorescence properties not only depend on the size factor (no. of atoms in a given cluster) but also on the interaction with surface adhered ligands present in the reducing/capping agent [187,188]. Capping agents such as ascorbic acid (dehydro-ascorbic acid form), bovine serum albumin (BSA) enriched with organic molecules, namely -OH,– SH, - NH_2, - COOH are found suitable during the development of nanoclusters in view of imparting them colloidal stability as well as making them hydrophilic & biocompatible [189,190].

Apart from stabilizing the surface of the developed nanostructure, ascorbic acid is a well-known reducing agent which holds the potential for managing resulting fluorescence intensity and rescuing the compromised BSA structure [191][192]. Furthermore, Bovine serum albumin (BSA), a non-glycosylated negatively charged template with several thiol groups (-SH) present in it, thus seamlessly coordinates with the surface of the nanoclusters by reducing their interfacial energy [193]. BSA acts as both a reducing and stabilizing agent during the synthesis of nanoclusters [37]. Predominantly, BSA protein being an excellent reducing agent, mediate the conversion of Mg^{2+} ions to metallic form Mg^{0} in the aqueous phase and affects the electronic band structure of the synthesized metallic clusters such that fluorescence properties could be tuned [3,85].

Incorporating the above-cited features of BSA/ascorbic acid, there has been very little work carried out earlier regarding the synthesis of magnesium nanoclusters. For example, Pandya et al., in their research, have reported the chemical synthesis procedure of fluorescent Mg-BSA nano-complex for cell-nuclei imaging [85]. The Mg-based nanocomplex was ~8.5 nm in size and resulted in blue and green colored fluorescent emissions. The in-vitro images acquired by nanocomplex were found to be poor in contrast and severely affected by autofluorescence arising from biological tissues within this spectral range. Therefore, it is highly desirable to synthesize Mg^{0} nanoclusters emitting in a broad spectral range (red, green, and blue) so that sharp or high signal-to-noise ratio images of biological cells can be acquired by employing these nanoclusters. Furthermore, the real-time applicability of these nanoclusters can be ascertained by possibly harnessing red light emission or a combination of red-green-blue light, capable of penetrating deep-lying tissues inside the body. It is important to mention here that, to date, white light-emitting (WLE) metallic magnesium nanoclusters have not been reported.

Therefore, herein we exclusively report the synthesis of biocompatible water-soluble white light-emitting (WLE) metallic magnesium nanocluster synthesized by a simple, affordable one-pot facile technique employing BSA and ascorbic acid. However, there are no reports on magnesium NPs being coated with ascorbic acid as a stabilizing agent. These nanoclusters show tunable fluorescent emission in the RGB region of visible light and collectively fluoresced as white light. Furthermore, the physicochemical characteristics of these developed nanoclusters have been examined using various spectroscopic techniques and successfully employed in the bioimaging of HaCaT cells (human keratinocyte cell line) using confocal microscopy.

3.2 Experimental Section

3.2.1 Material

Ultrapure deionized water was used throughout the process. 99.9% pure high-grade magnesium chloride salt ($MgCl_2$) and 99.9% pure L-ascorbic acid were purchased from Sigma Aldrich, and BSA protein was purchased from SRL. DMEM (Dulbecco's modified Eagle's medium), Streptomycin, and penicillin were obtained from CELL clone^{TM}, Genetics Biotech Asia Pvt. Ltd and Fetal Bovine Serum (FBS) was purchased from Gibco by life technologies. Trypsin-EDTA, MTT (3-(4, 5-dimethylthiazol-2-yl)-2, and 5 diphenyl tetrazolium bromide were purchased from Hi-Media. DMSO (dimethyl sulphoxide) was obtained from Merck Millipore. A tissue culture flask (surface area 25 cm^2, canted neck, vented cap) and 96 well plates (flat bottom) were purchased from Eppendorf. And 12 well and 6 well culture plates were obtained from Genetics Biotech Asia Pvt. Ltd. All the chemicals were purchased from commercial suppliers and used as received without any further modification and purification.

3.2.2 Characterization

Prepared FMNCs and their control were characterized by using various spectroscopic modalities. Fluorescence spectra were obtained with using PTI Quanta master 400 spectrofluorometer (Slit width = 1 nm, integration time = 0.1s and step size = 1nm). UV-visible absorbance spectra were recorded by using Elico SL210 spectrophotometer. The size analysis of the FMNCs was evaluated through High-resolution transmission electron microscopy (HR-TEM) on an FEI Tecnai G2 20 TWIN with an accelerating 200 KV electron beam voltage. Fourier Transforms Infrared Spectroscopy (FTIR) of prepared particles were examined with a Nicolet iS5 (THERMO electron scientific instruments LLC) using KBr pellets in the 4000 to 400 cm^{-1} range. The prepared FMNCs phase and crystallinity were estimated using Powder X-ray diffraction (XRD), Bruker, Model-D8 Advance (Eco). X-ray photoelectron spectra (XPS) were obtained using PHI 5000 Versa Probe III (Institute Instrument Centre, IIT Roorkee, Roorkee). Time-based measurements were performed with a vaFL920 Fluorescence life Time spectrometer using the TRES technique (Advanced Instrumentation Research Facility, JNU, Delhi). Mass spectra analysis was obtained using a MALDI-TOF Bruker (Autoflex speed) (Central Instrumentation facility, Department of Biosciences and Bioengineering, IIT Bombay, Mumbai). The cellular fluorescence behavior of FMNCs in HaCaT (Normal keratinocytes cell) was investigated by Carl Zeiss LSM 780 Confocal Microscope (National Facility for Laser scanning Centre, Zoology Dept. BHU, Varanasi) at 472, 541,595, and 636 nm. All measurements were conducted at ambient temperature if not noted otherwise.

3.2.3 Synthesis of FMNCs

All the glassware was washed by aqua regia (HCl (3): HN03 (1)), followed by gentle rinsing with DI water and ethanol two to three times. BSA templated magnesium

nanoclusters (FMNCs) were synthesized using $MgCl_2$ salt solution (10mM, 20.3 mg/ml, 10 ml) and BSA solution (450 mg/ml, 1 ml). Both the solution was mixed for 5 min (55° C, 900 rpm), followed by the addition of L-ascorbic acid (35 mg/ml, 3 ml). Subsequently, the solution was kept for 2 hrs at 55° C with constant vigorous stirring. After 2 hr of reaction, the solution color turned colorless to light yellow. Afterward, the solution was incubated at 55° C for 15 hrs. The solution color changed from light to pale yellow, indicating reaction completion. Prepared nanoclusters were centrifuged (15k rpm, 5 min) and kept at 4° C for further use. The reaction conditions were systematically optimized to achieve high fluorescence intensity. All possible control reaction was also performed under the same condition to investigate the fluorescent behavior.

3.2.4 Optimization of FMNCs

Effect of different processing parameters such as the amount of reducing agent, temperature, and pH of the medium, over the size, polydispersity, and intensity was evaluated. Initially, metal salt ($MgCl_2$) precursor was reduced by model protein BSA in an aqueous solution and then further stabilize by using ascorbic acid. It is important to notice that synthesis employed the use of naturally occurring ingredients in an affordable manner using the facile synthesis route. It was observed that there is a significant effect of processing conditions such as temperature, pH, reaction time, amount of reactant, reducing agent, and capping agent used on the fluorescence intensity of the FMNCs. The effect of all of the above processing parameters was studied as a function of FMNCs fluorescence intensity. Based on the highest fluorescence intensity, parameters and reaction conditions were systematically optimized. For example, 10 mM, 35 mg /ml, and 450 mg/ml, $MgCl_2$ salt, ascorbic acid, and BSA took respectively, highest FMNCs emissions were achieved.

An increase in reaction temperature up to 55°C yielded the highest, fluorescence intensity, further increase in temperature results in decreased fluorescence. It is anticipated that at temperatures higher than 55°C, the structure of BSA protein is affected adversely. While, reaction time and fluorescence intensity were found to be directly proportional and maximum fluorescence intensity is achieved for 17 hrs reaction time (2 hrs reaction time in hotplate with a stirrer, 15 hrs in an incubator). However, further increase in reaction time resulted in a decrease in blue emission, while red and green emissions increased, this enhancement in green and red emission is possibly due to increasing in nanocluster size or slow surface oxidation of FMNCs.

3.2.5 Cell Culture and MTT Assay

The cell compatibility assay of FMNCs was carried out by a colorimetric assay based on the conversion of the yellow tetrazolium salt MTT (3-(4, 5-dimethylthiazol-2-yl)-2, 5-diphenyl tetrazolium bromide) to purple color formazan crystals by reaction with mitochondrial succinate dehydrogenase of metabolically active cells. Cytocompatibility of FMNCs and their control (Cell Media) were determined on HEK-293 (human embryonic kidney cell line) as well as human breast cancer cells (MDA-MB-231). The cell lines were maintained in high glucose complete DMEM (complete medium consisting of 10% FBS, supplemented with 20 mM L-glutamine, 100 units/mL penicillin, and 100 µg/mL streptomycin) at 37 °C and 5% CO2 in a humidified atmosphere. Briefly, 1×10^4 HEK-293 and MDA-MB-231 cells per well were seeded in two different 96 well plates and incubated for 24 hrs for adherence. After 24 hrs, the span medium was replaced by fresh DMEM containing various concentrations (1/10 th, 1/100 th, 1/1000 th of 30 mg/ml stock) of FMNCs, followed by incubation for 24 h in a 5% CO2 humidified atmosphere.

The medium was then removed, and 100µL of fresh medium containing 5 mg/mL MTT solution was added to each well and incubated further for 2 h. Finally, the MTT solution was removed, and 100µL DMSO was added into each well to dissolve the formazan crystal, followed by incubation in the dark at 37 ºC for 30 minutes. The intensity of the color developed was assayed using a Micro ELISA plate reader at 570 nm. The cell viability was estimated according to the following formula: -

% Cell viability = [O.D of FMNCs treated cells/O. D of Control cells] ×100

3.2.6 Cell Imaging

The cellular fluorescence of FMNCs was detected by confocal microscopy. The normal cell line of keratinocytes (HaCaT) was seeded in 6 well culture plates having coverslip in a complete medium with a density of 2×10^4 cells per well. After 24 hrs, the seeded cells were treated with a 1/10 th ratio of freshly prepared FMNCs (30 mg/ml stock) with the complete medium and incubated further for 24 hrs at 37°C in humidified 5% CO_2 incubator. After 24 hrs, adhered cells on coverslips were taken gently from the spent medium. Finally, the cells were fixed using 4% formaldehyde and imaged under confocal microscopy to study the fluorescence property of the FMNCs.

3.2.7 MALDI-TOF

Bruker Autoflex speed Matrix-assisted laser desorption/ionization-time of flight facility used sinapinic acid as the matrix. The sample was ionized with the pulsed nitrogen laser of 337 nm. Mass spectra were recorded in the positive linear mode with an average of 500 shots for each spectrum. The 1 ml of a matrix was prepared by dissolving 10 mg of sinapinic acid in a solution containing 500 µl acetonitrile and 500 µl 0.1% trifluoroacetic acid. The sample for spotting purposes was prepared by mixing 1µl of FMNCs sample and 1µl of

matrix and then spotted onto the target plate. Sample (FMNCs) dilution was done with ultrapure Milli-Q water.

3.2.8 Fluorescence Lifetime

The lifetime measurement of FMNCs and BSA protein were performed using the time-resolved fluorescence spectrometer (TRFS) technique. The sample (FMNCs and BSA) was excited by a 375 nm, 496 nm Laser, and 598 nm LED light source. Spectra were recorded at 10,000 counts, and on account of maintaining the sample, ambient temperature at 25°C the fluorescence lifetime setup was linked with the external circulation water bath. The recorded lifetime data were optimized using a tri- exponential curve owning to get the chi-square values near 1.00 with the help of *Decay Fit 1.4* software.

3.2.9 Quantum Yield

The quantum yield measurement of the FMNCs for green and blue emission was conducted relative to the standard fluorophore Rhodamine 6G and quinine sulfate; its quantum yield is found at 0.95 in ethanol and 0.55 in 0.1M H_2SO_4, respectively. The Quantum yields are calculated with the help of the following equation [194].

$$Q_{sm} = Q_{rf} \times \frac{I_{sm}}{I_{rf}} \times \frac{A_{rf}}{A_{sm}} \times \frac{{\eta_{sm}}^2}{{\eta_{rf}}^2}$$

Where Q_{sm} is the quantum yield of FMNCs, $Q_{rf\,is}$ the quantum yield of reference, I_{sm} is the area under the PL curve of FMNCs, I_{rf} is the area under the PL curve of reference, A_{rf} is the absorbance of the reference, and A_{sm}, is the absorbance of the FMNCs, whereas η_{Sm} and η_{rf} is the refractive index of the FMNCs and reference respectively. Thus, the quantum yield of FMNCs for blue and green emissions was calculated at 1.2 % and 4.6 %, relative to the quantum yield of quinine sulfate and rhodamine 6G, respectively (Figure. 3.7 a, b).

3.3 Result and Discussion

The vacuum dried (60°C for 12 hrs) nanoclusters were ground and used for further characterizations (XPS, FTIR, and XRD). In contrast, the aqueous solution was utilized for HR-TEM, MALDI-TOF, MTT, confocal, lifetime, and fluorescence spectroscopy analysis. The electron microscopy was performed using 10 times diluted FMNCs solution for drop casting on a copper grid (Room Temperature drying).

3.3.1 Fluorescence spectroscopy and UV-Vis Spectroscopic characterization

Fluorescence spectra of nanoclusters and their controls were acquired using a spectrofluorometer. The aqueous suspension of FMNCs confirmed fluorescence emission at 450 nm (blue), 536 nm (green), 565 nm (yellow), and 620 nm (red) on 366, 469, 516, and 560 nm excitation, respectively (Figure.1). Furthermore, upon 366 nm excitation, a continuous emission spectrum ranging from 400-620 nm with full width at half maximum (FWHM) of 120 nm, resulting white light emission (Figure. 3.1a). This is also corroborated by the fact that the Commission Internationale de I'Eclairage (CIE) color index for the spectrum is found to be (0.32, 0.33) when excited in ultraviolet light (Figure. 3.2a). Notice that for pure white light, CIE is found to be (0.33, 0.33) [39]. Previous work by Pennycook et al. [172] on nanoclusters has demonstrated that the continuous emission of white light emerging from nanoclusters as a continuous spectrum on UV excitation is due to fluxional states of the intrinsically disordered atoms loosely arranged in the nanocluster. Additionally, the obvious excitation-dependent emission from nanoclusters cannot be neglected. It is important to assert that the MALDI-TOF results show the presence of 28-1394 atoms large nanoclusters.

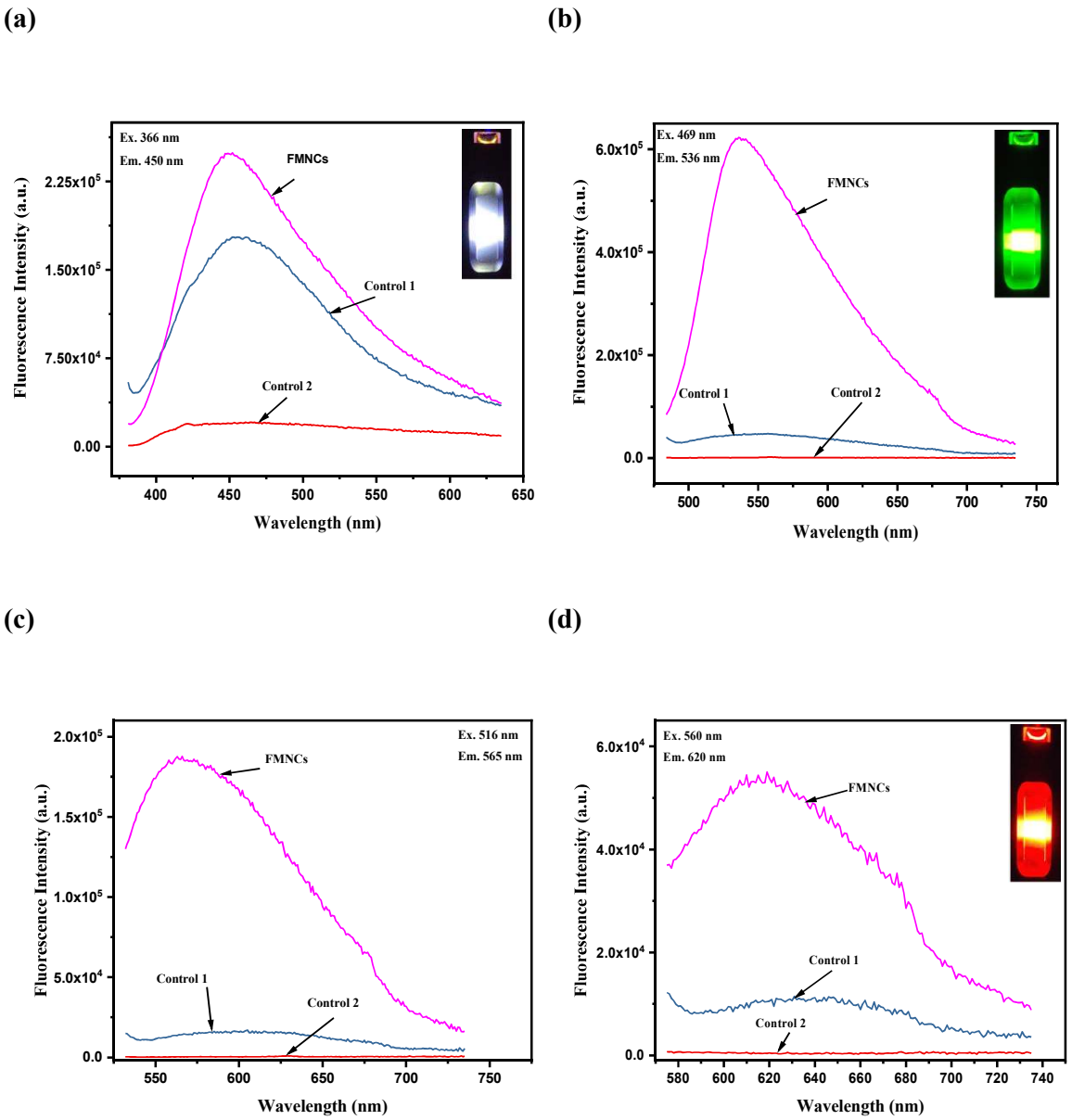

Figure. 3.1 The fluorescence emission spectra of FMNCs (30 mg/ml) and controls (Control 1: $MgCl_2$ salt + BSA protein (31 mg/ml); Control 2: $MgCl_2$ salt + ascorbic acid (8.37 mg/ml) at (a) The optimal excitation and emission spectra (λ_{Ex}. 366 nm / λ_{Em}.450 nm) of FMNCs and control and its inset image shows aqueous FMNCs colloid under 366 nm excitation. (b) the excitation and emission spectra (λ_{Ex}. 469 nm / λ_{Ex}. 536 nm) of FMNCs and its control and its inset image shows aqueous FMNCs colloid under 469 nm excitation. (c) Excitation and emission spectra (λ_{Ex}. 516 nm / λ_{Em}. 565) FMNCs and its control (d) excitation and emission spectra of FMNCs and its control at λ_{Ex}. 560 nm and λ_{Em}620 and the inset image shows aqueous FMNCs colloid under 560 nm excitation.

Furthermore, TEM analysis of FMNCs was observed to be 1.62 ± 0.62 nm large in size (sample size 100 nanoclusters). As per previous reports [195], even a slight difference in particle size may result in significant changes in the energy level separation leading to different emission wavelengths due to energy discretization [124,196]. Also, it is important to note that none of the controls (i) $MgCl_2$ + ascorbic acid (8.36 mg/ml stock) and (ii) $MgCl_2$ + BSA (31 mg/ml stock) fluoresced under the same excitation, except $MgCl_2$ + BSA, (fluoresced in blue region) due to the presence of endogenous tryptophan residue (Trp-134, and Trp- 213) [197–199] (Figure. 3.1). However, it is observed that the same reaction mixture is further allowed to react in the incubator and coagulates while the $MgCl_2$ + BSA + Ascorbic acid (30 mg/ml stock) mixtures remain as it is (Figure. Appendix-A1 a). Our observations demonstrate that using simple one-pot synthesis, white light emitting Mg^0 nanoclusters (solution as well as in powder) (Figure. 3.1a inset and Figure. 3.2b inset) can be prepared. The combination of RGB colors producing white light could be efficiently utilized for multicolor bioimaging with the help of optical filters. Subsequently, red and green emissions were used here for deep tissue imaging [200].UV-Visible measurements were performed to gain further insight into the interaction between Mg, BSA, and ascorbic acid. A typical UV-Vis absorption spectrum of an aqueous BSA and FMNCs is acquired and displayed in Figure. 3.2d. The Figure are shows a sharp absorbance band at 280 nm of BSA solution, indicating the presence of disulfide bonds and aromatic residues [201],[202]. At the same time, FMNCs solution displayed a hypochromic shift in the absorbance band (280 nm → 264 nm) concerning the BSA solution indicating the interaction between BSA and ascorbic acid, which led to a decrease in the hydrophobicity in the microenvironment of the aromatic residue, this phenomena is in line to our proposed mechanism [203][44].

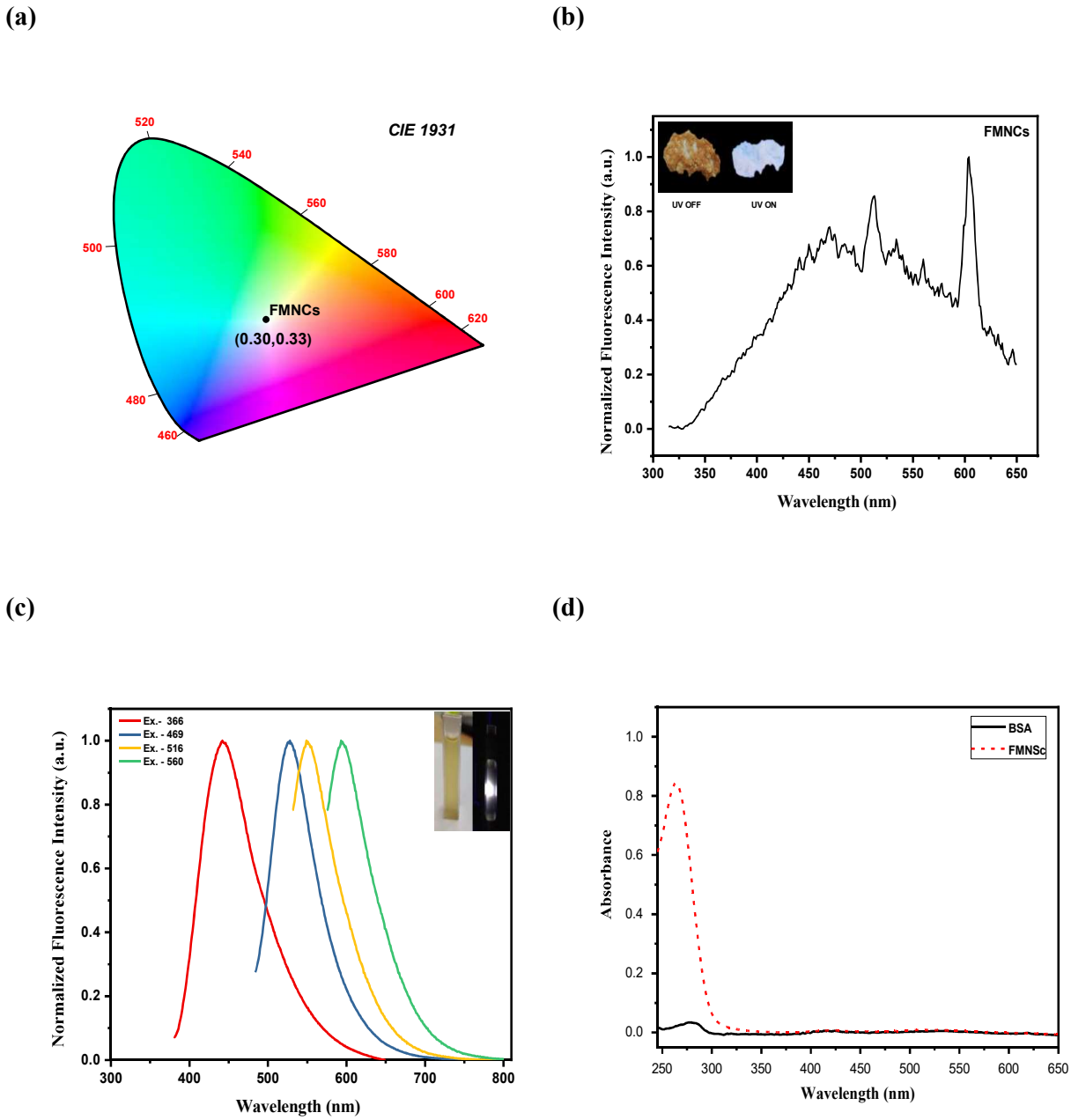

Figure. 3.2 (a) CIE chromaticity diagram of FMNCs shows the coordinate (0.30, 0.33) as the single emitter at 300 nm excitation. (b) The normalized photoluminescence intensity spectra of FMNCs at 300 nm excitation and the inset image shows lyophilized FMNCs powder with and without UV excitation (one-year-old) (c) Excitation wavelength-dependent broad emission spectra of FMNCs. (d) UV-Vis absorption spectra of native BSA and FMNCs.

Furthermore, the disappearance of the peak at 300-400 nm range, accompanied by an absence of magnesium ion hinting the complete conversion of $Mg^{2+} \rightarrow Mg^{0}$ (shown in Figure. 3.2d). However, more detailed studies like surface and infrared spectroscopy are required to completely decipher the chemical composition of the ultrasmall particles formed during synthesis.

3.3.2 Surface and Infrared Spectroscopy

The combined Fourier transform infrared spectroscopy (FTIR) and X-ray photoelectron spectroscopy (XPS) data analysis can provide the chemical constitution of FMNCs, the interaction responsible for its stabilization, and associated fluorescence. Therefore, XPS spectra of FMNCs are initially acquired (Figure. 3.3 b). The XPS spectra of carbon peak (284.6 eV) is adjusted and deconvoluted [204],[205],[206]. Deconvoluted C 1s spectra of FMNCs indicated two prominent peaks at 284.6 and 286.4 eV, attributed to C-C and C=O bonds, respectively. While Mg 2s and 1s state displayed prominent peaks at 88.6 eV and 1303.5 eV suggesting the formation of metallic magnesium (Mg^{0}) [207],[208] (Figure. 3.3 c, Figure A3 d). Besides, the absence of a 93.0 eV peak in the Mg 2s spectra in the FMNCs, clearly indicated the absence of Mg^{2+} species in the sample [209].

Furthermore, the absence of a peak at 1305.3 in the Mg 1s spectra suggested the absence of oxidized magnesium [210,211]. The XPS analysis, therefore, clearly indicates the formation of fluorescent Mg^{0} nanoclusters (FMNCs). Based on earlier reports which indicated the formation of Mg^{0} nanoparticles due to reductive properties of BSA[3,85] and opening of BSA structure in acidic conditions [191,212,213]. It is anticipated that, at the time of reaction between $MgCl_2$ and BSA, the opening of the protein strand in the acidic medium and electrostatic interaction with Mg^{2+} ions occur [3]. At the same time, it is assumed that ascorbic acid, interacting with hydrophobic pockets of BSA proteins, releases

two electrons forming the DHAA molecule [192], which is also an excellent capping agent [189]. Previous studies have also demonstrated that ascorbic acid interaction with hydrophobic groups of BSA helps reclaim its structure by donating an electron and also enhances fluorescence [191,192]. In concurrence with the previous report, we also observed that when $MgCl_2$ reacted with BSA, 360 nm big nanoparticles (Figure. A1 c) were formed. However, on further addition of ascorbic acid, the same nanoparticles were reduced to 10 folds smaller size (~30 nm), as shown in Figure. A1 d. At the same time, nanoclusters displayed enhanced fluorescence (as shown in Figure. 3.1), excellent hydrophilicity, and demonstrated good stability. Note that previous studies have also reported similar observations [63]. Still, detailed studies are required to support our hypothesis completely, which is currently out of the scope of this manuscript. Although XPS studies indicated the formation of Mg^0 nanoclusters, further analysis pertaining to carbonyl or other groups needs to be analyzed, which will indicate the interaction of protein and ascorbic acid with Mg^0 nanoclusters; therefore, O1s spectra of FMNCs were acquired and analyzed.

The O 1s spectra displayed a peak at 531.4 eV, which can be attributed to the carbonyl (C=O) functional group [214,215]. Moreover, the S 2p spectrum indicated peaks at 162.5, 162.6, eV, attributed to chemisorbed low coordinated divalent sulfide ions (S^{2-}) to the FMNCs surface [46]. In contrast, the third peak at 163.8 eV indicated the formation of the metal-sulfur bond [216], [217], [218]. It is important to note that the presence of a 163.8 eV peak in the S 2p state indicates the formation of metal-thiolate bonding and, thereby, the interaction of BSA and nanocluster surface, which is in line with our proposed design rationale. The metal-thiolate interactions reduce the surface free energy and stabilize the nanoclusters [219]. Most importantly, absences of 169.2 eV peak corresponding to S2p (follow the representational norm) suggest that sulfur did not oxidize, so protein degradation is ruled out [169]. Furthermore, the visible peaks of Na (1s), O (1s), C (1s),

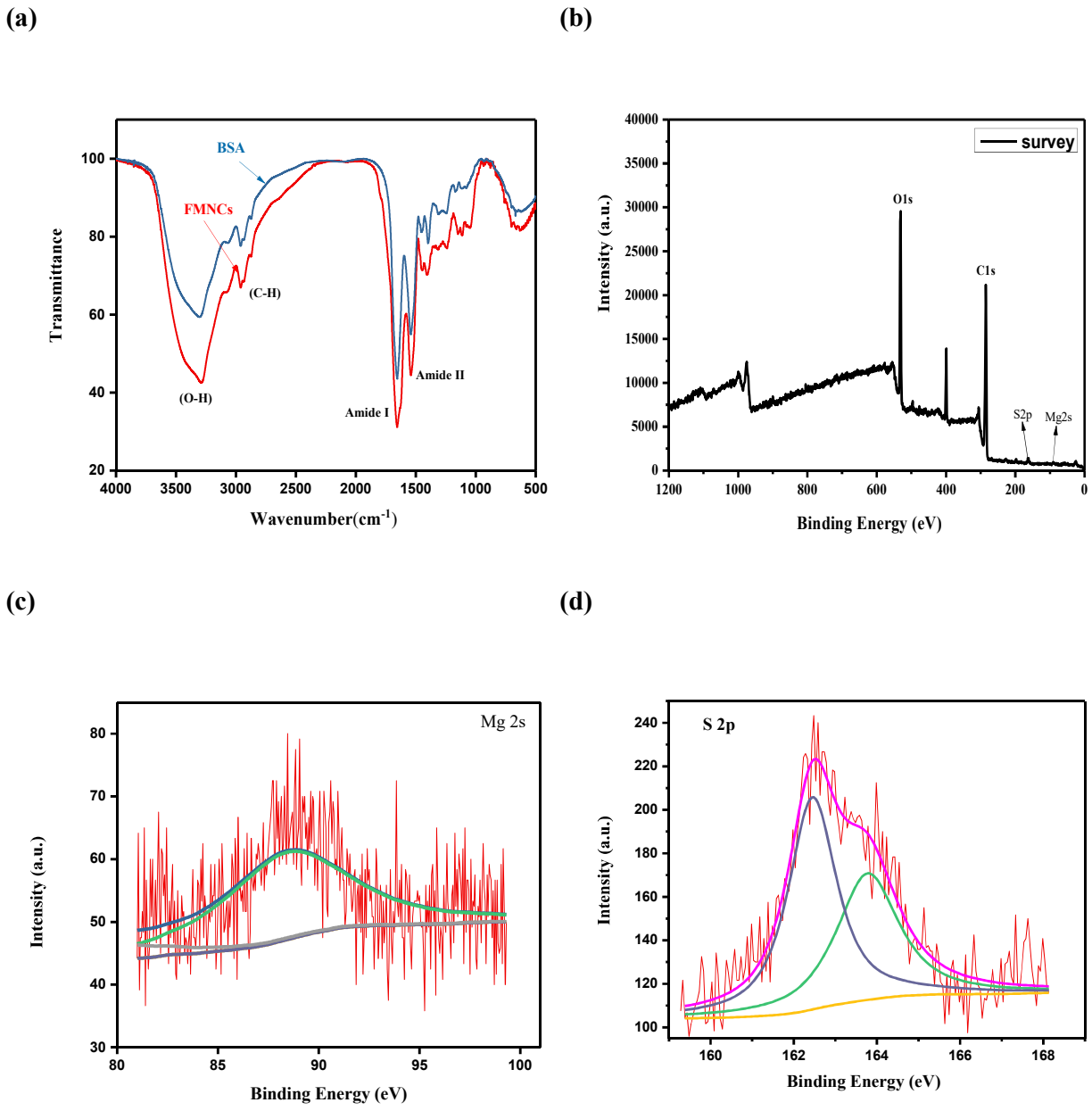

Figure. 3.3 (a) FTIR spectra of FMNCs and BSA protein,(b) XPS Survey data, (c) Mg 2s, (d) S 2p.

and S (2p) in the spectra can be attributed to the presence of BSA protein scaffolding in the FMNCs [87],[169] (Figure. 3.3 c, d), and Figure. Appendix-A2 (a, b and c).

The FTIR spectra of BSA and FMNCs powder are acquired (Figure. 3.3 a). The FTIR spectra of BSA indicated the presence of three amides bands, amide I (1600-1700), amide II (1480-1575), and amide III (1229-1301), attributing to C=O stretching, N-H bending,

and the combination of CN stretching, C=O bending, and C-C stretching respectively [220], [169], [221]. It is important to note that early reports have demonstrated the presence of multi-functional moieties stabilizing the nanoclusters. Furthermore, no significant difference in FTIR spectra of FMNCs and BSA protein is observed except change in their relative intensities. The spectral intensities of amide I peak (1654 cm^{-1}, free BSA) and amide II (1541 cm^{-1}, free BSA) were significantly reduced in the FMNCs, indicating an interaction of Mg^{+2} with C=O, COO-, and N-H group of BSA. Further, the binding interaction of Mg^{+2} with BSA protein was revealed by the band shifting of the amide A band from 1654 cm^{-1}→ 1655 cm^{-1}, this shifting was due to the interaction of Mg^{+2} ions with the C-N and N-H groups of protein,[222] whereas the reduction in the spectral intensities of the amide I band suggested a significant decrease of α helix in the secondary protein structure [222]. However, the slight shift in the FMNCs spectra from 3306 cm^{-1} → 3291 cm^{-1} concerning the BSA can be attributed to the amide (C=O) band, which indicates the successful grafting of protein on the nanocluster surface [223]. Additionally, compared to BSA protein, a significant decrease in FMNCs spectra suggested conformational changes due to nanoclusters formation [221],[224]. In general, it is observed that the spectra of the nanoclusters are broader than that of protein [221]. Further, studies were performed to estimate the size and phase and analysis of Mg^0 nanoclusters.

3.3.3 Size and Phase Analysis

Figure. 3.4 shows the electron microscopy and MALDI-TOF data, indicating the size of FMNCs. The TEM images (Figure. 3.4 a) indicated the formation of as big as 1.62 ± 0.62 nm FMNCs (sample size=100) normally distributed (Gaussian) (Figure. 3.4 b) over the grid.

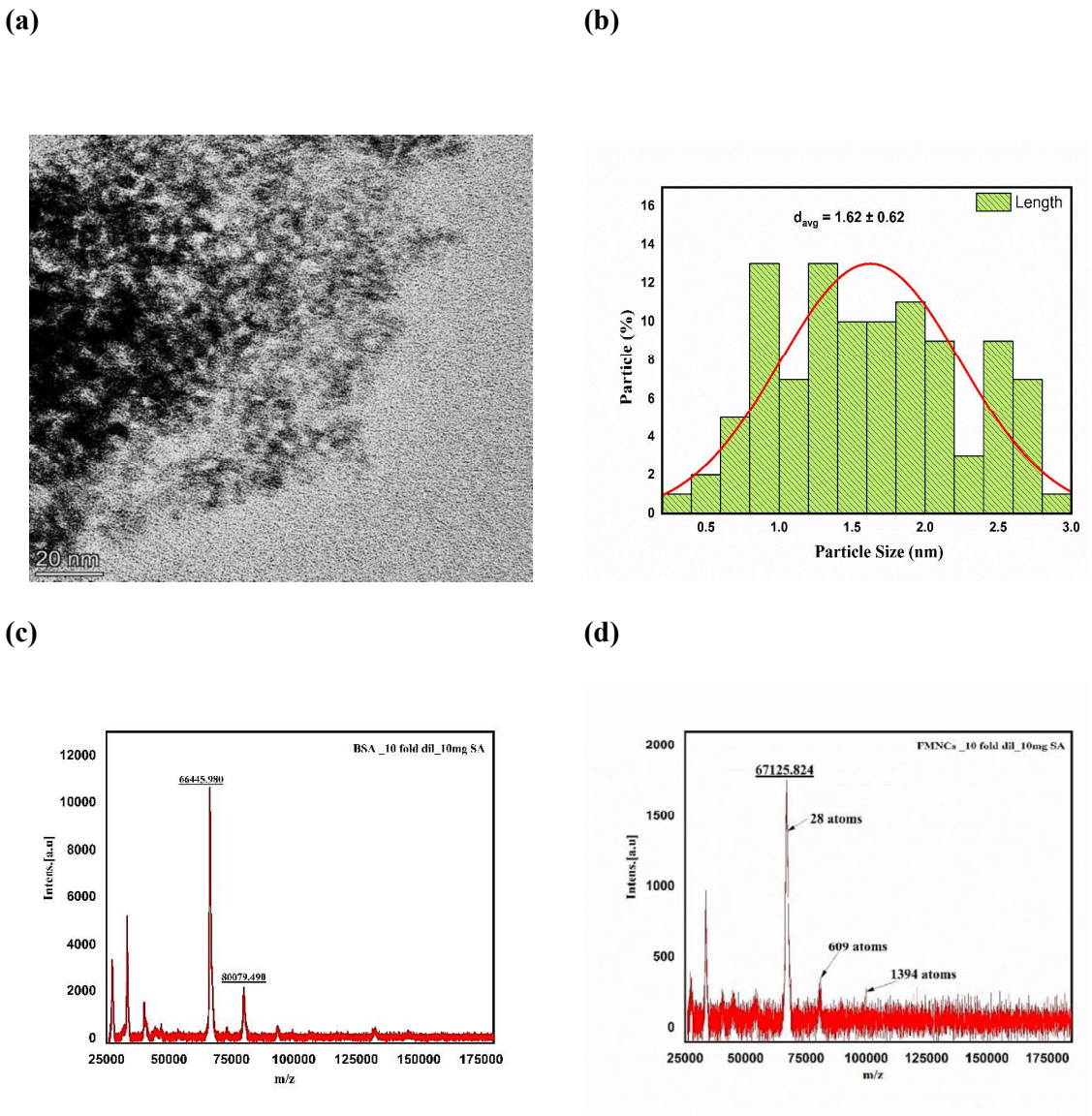

Figure. 3.4 (a) HR-TEM image of the FMNCs at 20 nm scale bar (b) Particle size distribution curve, which was calculated using TEM image. (c) MALDI-TOF spectra of BSA, (d) MALDI-TOF spectra of FMNCs.

The number of Mg atoms was evaluated by calculating the shift in the molecular weight of marker protein (BSA) (Figure. 3.4 c) and the FMNCs. The MALDI-TOF results of FMNCs displayed 67126, ~81064, and 99920 Da peaks attributed to the formation of 28, 609, and 1394 atom big Mg nanoclusters (Figure. 3.4 d).

Interestingly, calculations based on TEM size analysis yielded 33 atoms of big FMNCs, which is quite close to estimated values from MALDI-TOF. Furthermore, FMNCs were investigated for phase purity and crystallinity using XRD analysis. The XRD analysis of native BSA (~9°, 19.5°, and 29.5°) and BSA templated FMNCs (19.5° and 29.5) displayed similar peaks (Figure. 3.5), which is due to BSA only and suggests no phase change.

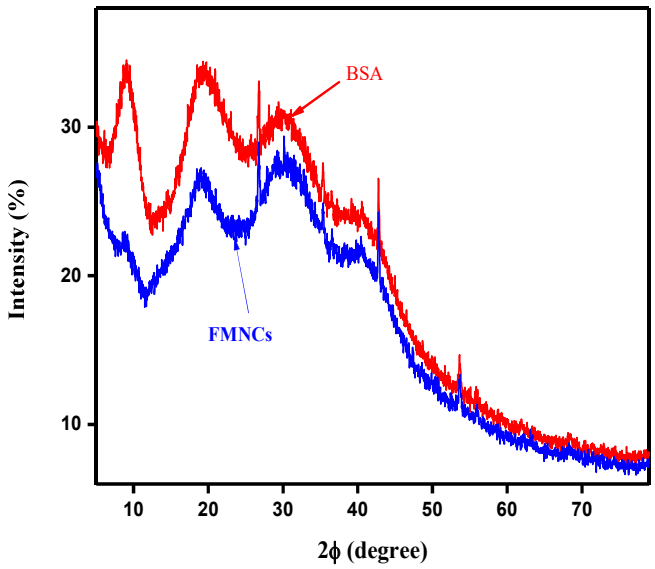

Figure. 3.5. XRD spectra of BSA and FMNCs.

It is observed that with the progress of FMNCs, the peak at ~9° (inherent to BSA) disappeared, due to metal-thiol interaction, decreasing the BSA crystallinity[225][175,191]. Moreover, previous studies have also demonstrated that such data may indicate the successful grafting of Mg^0 nanoparticles within the protein matrix.

3.3.4 Lifetime Analysis

To gain insight into the fluorescence mechanism, lifetime measurements of FMNCs and BSA in an aqueous medium are acquired, and data is fitted into a tri-exponential decay curve and analyzed.

Data showed an average lifetime of 5.45, 3.85, and 0.55 ns for BSA, corresponding to 375, 496, and 598 nm excitations. For FMNCs, 2.94, 3.07, and 0.30 ns (Table 3.1) were the average lifetimes for the same excitation wavelength (Figure. 3.6, Figure. Appendix-A3 a, b). Notice that lifetime measurement for different wavelengths emanated from the single sample. Here it is noteworthy that the lifetime decay and energy of excitation wavelength are related to each other because from the literature it observed that higher excitation energy resultant a longer lifetime [226]. It is interesting to note that single pot synthesized FMNCs showed luminescence in the RGB region, subsequently producing white light, all from one sample. To date, only a few reports have demonstrated white light-emitting nanoclusters prepared in a single step and one pot. White light emission from the FMNCs could be due to different sizes of nanoclusters in the sample. Earlier studies have demonstrated that the presence of different-sized nanoclusters in the same sample solution [227] yields different lifetimes and emissions [228]. While other studies have shown decreased lifetime as the increase in the size [228] of the protein templated nanomaterials occurs.

System	α_1	τ_1 (ns)	α_2	τ_2 (ns)	α_3	τ_3 (ns)	τ_{avg} (ns)	$\chi 2$
Blue FMNCs	0.67249	0.38692	0.04412	6.51208	0.28339	2.41446	2.94	1.620
Green FMNCs	0.27488	2.20788	0.16321	4.30939	0.556191	0.21820	3.07	1.053
Red FMNCs	0.00150	1.63545	0.00043	3.20560	0.99807	0.02660	0.30	1.197
[*] BSA	0.30941	3.11485	0.06844	10.44459	0.62215	0.41721	5.45	1.35
[**] BSA	0.81530	0.14107	0.03162	7.84242	0.15308	2.12673	3.85	1.44
[***] BSA	0.00251	1.53032	0.99669	0.02728	0.00080	3.92062	0.55	1.19

Table 3.1 Fluorescence lifetime of FMNCs and Processed BSA

[*] BSA corresponds to excitation by 375 nm laser with a blue emission, [**] BSA denotes excitation by 496 nm laser with green emission, [***] BSA denotes excitation by 598 nm LED lamp with red emission. Tavg = $(\alpha_1\tau_1^2 + \alpha_2\tau_2^2 + \alpha_3\tau_3^2) / (\alpha_1\tau_1 + \alpha_2\tau_2 + \alpha_3\tau_3)$ denotes average lifetime, whereas, $\chi 2$ represent extent of fitting among the model and experimental.

Interestingly, our studies have indicated a lower lifetime (0.3 ns) for red emission and the highest (3.07 ns) for green color emission. It is understood that lifetime shortening may be due to three possibilities: (i) fluorescence resonance transfer (FRET), (ii) surface energy transfer (SET), and (iii) electron transfer. Phenomena of FRET are known to occur when there is an overlap between the emission and absorption spectra of donor and acceptor, respectively, and their separation is less than 10 nm; however, there is no apparent spectral overlap between donor protein and acceptor metal, and therefore this mechanism is

excluded [228]. Whereas surface energy transfer (SET) phenomena take place for larger donor and acceptor separation distances (10 nm or more), and there is no prerequisite for spectral overlap [228]. It is important to notice that, in the current case, the BSA molecule is closely interacting with the surface of the FMNCs, and therefore SET can be overruled. Besides, the overall size of the FMNCs is smaller than 15 nm. Besides, it is important to note that fluorescence lifetime is inversely proportional to the size of the nanoclusters [6,22,23], which is evident from MALDI-TOF results. Due to polydispersity, different excitation may result in different emissions, which is visible in the results (Figure. 3.1). Although detailed studies are required to support our statement.

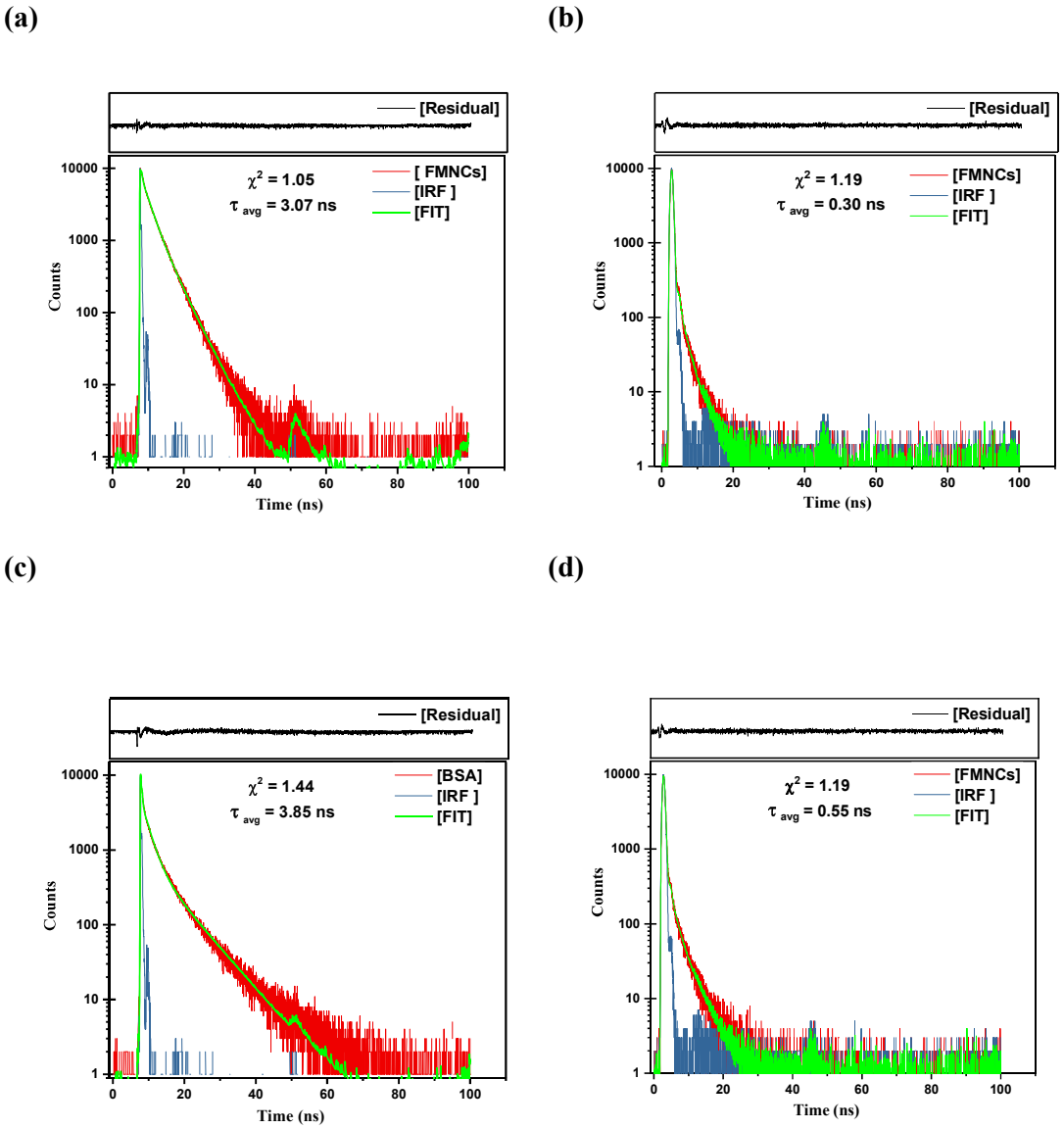

Figure. 3.6. (a) Fluorescence lifetime decay profile (λ_{Ex} 496 nm/λ_{Em} 564 nm) of FMNCs (b) Fluorescence lifetime decay profile (λ_{Ex} 598 nm/λ_{Em} 658 nm) of FMNCs (c) Fluorescence lifetime decay profile (λ_{Ex} 496 nm/λ_{Em} 564 nm) of Processed BSA (d) Fluorescence lifetime decay profile (λ_{Ex} 598 nm/λ_{Em} 658 nm) of Processed BSA.

The absorbance studies of FMNCs showed a direct bandgap of 4.21 eV and an indirect bandgap of 4.11 eV (Figure. 3.7 c,d)), which is slightly higher than prenucleation calcium carbonate nanoclusters reported by our group (Shivesh et al.) [183]. Also, early studies on MgS nanoclusters were shown to have an indirect bandgap of 4.2 eV. [229]

It was observed that the MgS bandgap varied from 4.0 – 4.80 eV. [230],[231],[232],[233],[234]. Furthermore, it is observed that the absorbance shifts from 280 nm → 264 nm, as compared to the pure aqueous BSA solution, indicating three possibilities (i) formation of ultrasmall-sized nanocluster or (ii) electron transfer occurring between the tryptophan residue (BSA) and FMNCs, or (iii) both. Interestingly, the synthesis of ultrasmall FMNCs has already been shown by our TEM and MALDI-TOF studies. While a small lifetime of the FMNCs as compared to BSA may be indicative of electron transport between tryptophan and FMNCs surface [228]. Therefore, both electron transfer and size reduction may play a key role in the blue-shifting of FMNCs absorbance spectra. Besides, as XPS corroborates, metal-thiolate bond (Mg-S) formation may play a crucial role in Ligand metal charge transfer. Most importantly, we observed that on substitution of PVP polymer in place of BSA (same protocols), FMNCs generated only blue, green fluorescence (Figure. Appendix-A5) indicating ligand-dependent emission from the nanocluster and hence Ligand to Metal Charge Transfer (LMCT) is anticipated to be the responsible mechanism of fluorescence in developed FMNCs [165].

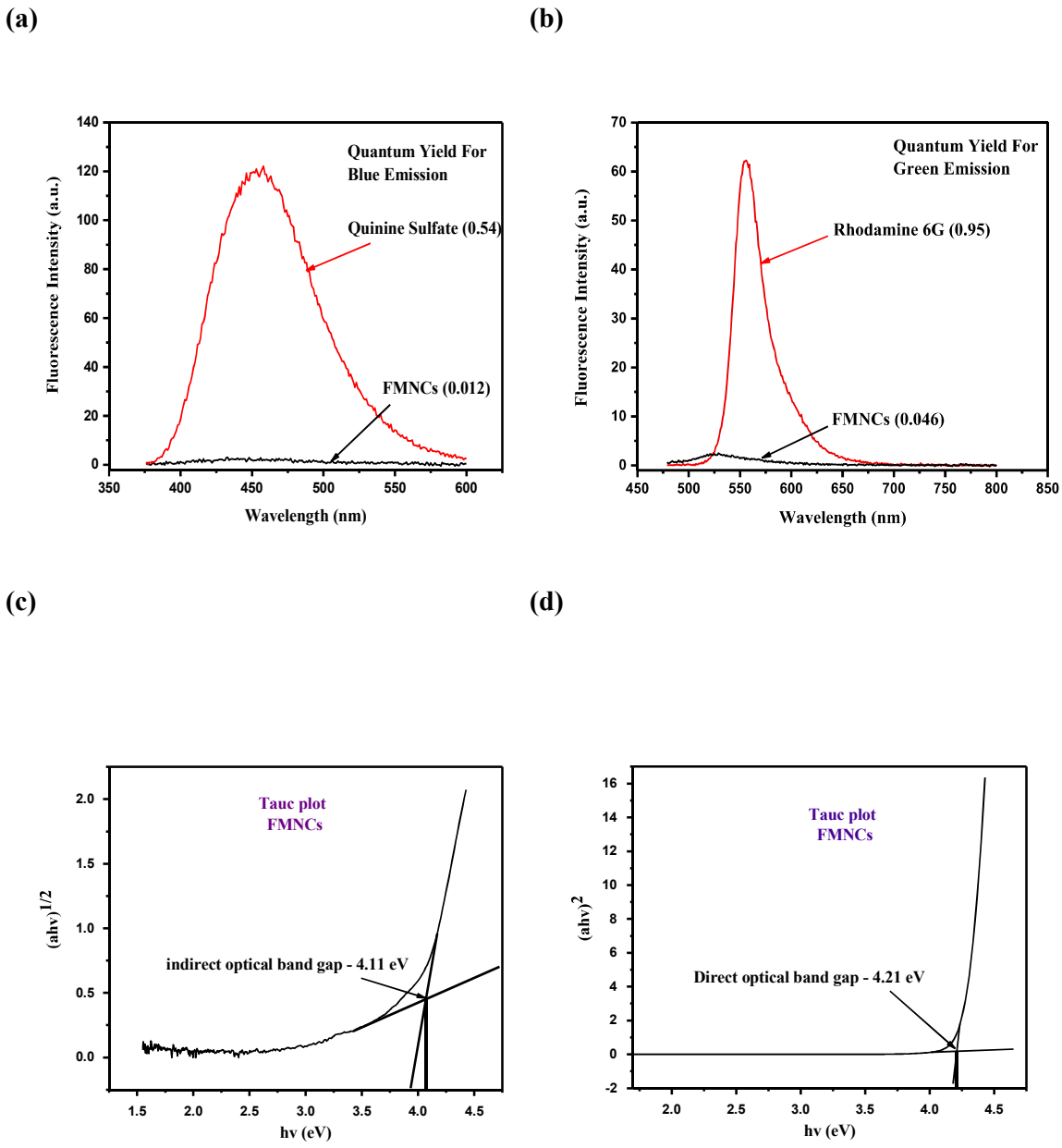

Figure. 3.7. (a) Fluorescence spectra of FMNCs and Quinine sulfate as reference at 366 nm excitation value, under the same absorbance value (<0.5). (b) Fluorescence spectra of FMNCs against rhodamine 6G at 469 nm emission. (c) Indirect optical band gap energy of FMNCs. (d) Direct optical band gap energy of FMNCs.

3.3.5 Stability of FMNCs

The stability of FMNCs as a function of fluorescence intensity is a performance indicator. During bioimaging, samples containing nanoclusters are often under continuous excitation, leading to permanent or temporary loss of fluorescence. Besides, prolonged storage of nanoclusters (aqueous and lyophilized form) also results in unwanted aggregations resulting in fluorescence loss in several cases. Therefore, the stability of FMNCs is evaluated in an aqueous solution as well as in lyophilized powder (One year old) when stored at 4℃ (Figure. Appendix-A4 a). It is observed that synthesized FMNCs retained their fluorescence (lost 20-30% of its original intensity) even after 8 months to 1 year of storage (at 4°C) in an aqueous and as well in powder form, respectively (Figure. Appendix-A6).

It is important to note that strong interaction between the electron-donating N- atoms (BSA) and the surface atoms of the FMNCs [165] prevented the surface oxidation of Mg^0 nanoclusters resulting in enhanced spectral as well as shelf-life stability [225,235]. Furthermore, it is observed that even adding freshly prepared NaCl solution in different concentrations (as high as 300 mM) did not alter its PL intensity, indicating excellent ionic tolerability (Figure. Appendix-A4 b).

The photostability of nanocluster is one of the crucial properties used in biolabeling and imaging purposes. Therefore, photostability experiments were performed to examine the fluorescence behavior of FMNCs under the Xe-lamp source (inbuilt to the spectrofluorometer) for a prolonged period (Figure. 3.8a). This experiment was performed in the diluted (OD > 0.5) FMNCs colloidal solution for 82 minutes at different emissions such as 450 nm, 536 nm, 565 nm, and 620 nm.

(a) **(b)**

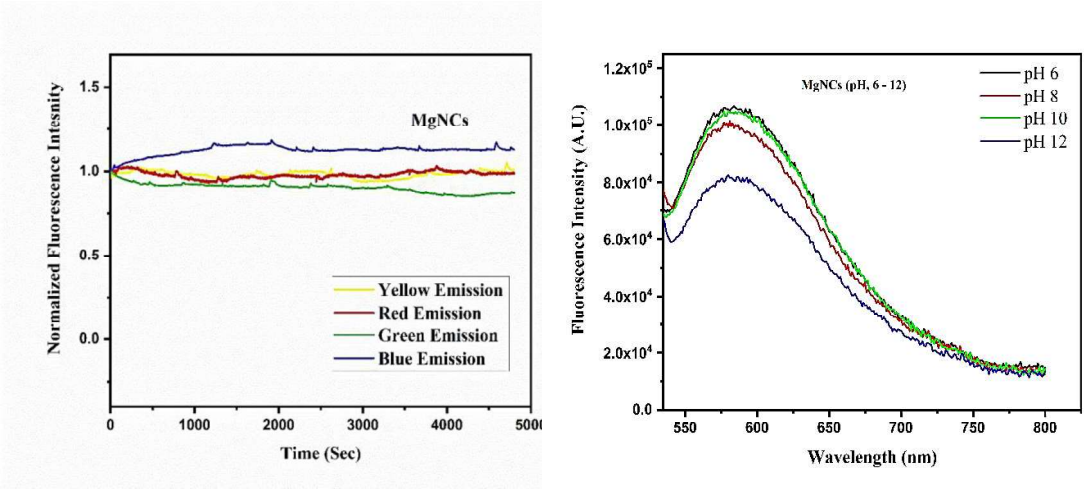

Figure. 3.8 (a) Photostability of FMNCs at different excitations (366, 469, 516 and 560) (b) ph. Dependent Fluorescence emission spectra at different pH. (6,8,10 and 12) Values, The pH. of the parent medium was 4.0.

The time-dependent spectra revealed the absence of any significant drop in fluorescence even after prolonged exposure to intense light (Figure. 3.8a). This study suggested that the prepared FMNCs were potential candidates for imaging and labeling purposes and could become better substitutes for expensive dyes.

3.3.6 Application of FMNCs

Lab synthesized FMNCs were further used for bioimaging in HaCaT cell lines. Before its applications as a bioimaging label. These nanoclusters (FMNCs) were tested for cytocompatibility in different cell lines, such as HEK 293 and MDA-MB-231, for practical usage. After completion of the cytocompatibility assay, FMNCs were incubated with cell lines, and confocal images were acquired.

3.3.7 Cytocompability (MTT assay) and Bioimaging

To investigate the cytotoxic behavior of prepared FMNCs, 3-(4, 5-dimethylthiazol-2-yl)-2, 3-diphenyl tetrazolium bromide (MTT) assay was performed on a normal cell line (HEK-293) as well as breast cancer cell line (MDA-MB-231). The viability assay was performed for FMNCs at (1/10 th, 1/100 th, 1/1000 th) dilution of the stock solution (30 mg/ml). Figure. 3.9 (a,b) shows cell viability for control (culture media) and FMNCs treated cell lines. Results of the MTT assay suggested that FMNCs did not induce toxicity in both the cell lines; in contrast, they represent highly biocompatible FMNCs in human embryonic kidney cells (HEK-293) and epithelial human breast cancer cell line (MDA-MB-231) even at high concentrations. The increased value of cellular viability of HEK-293 cells compared to control in a concentration-dependent manner (more than 100%) reflects the increase in cell proliferation within the stipulated incubation period, and these nanoclusters were also found to be biocompatible in MDA-MB-231 cells. These results indicate that FMNCs are biocompatible nanoclusters that can be safely used for bioimaging applications in both normal and cancerous cell lines without altering the integrity of cell lines. MTT results also suggested that the FMNCs could be a potential candidate for wound healing application.

(a) **(b)**

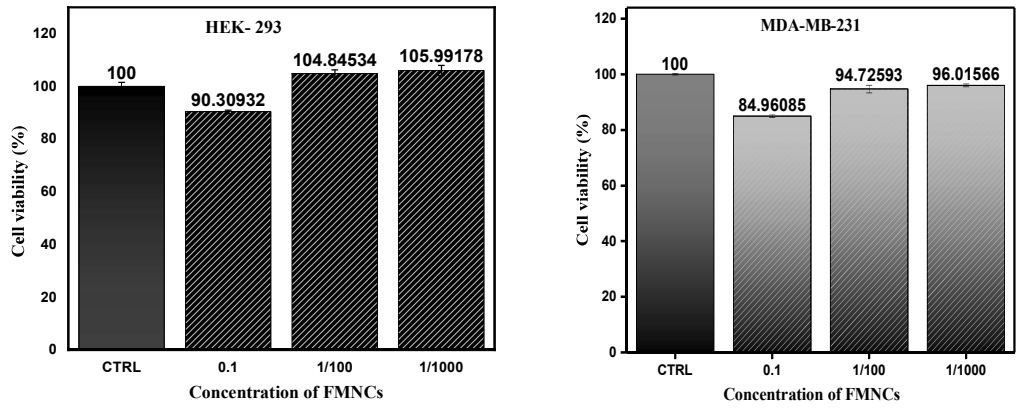

Figure. 3.9 (a) Cell viability measurement, followed using MTT assay of HEK-293 cells treated with different concentrations of FMNCs (stock concentration 30 mg/ml). (b) Cell viability assay of FMNCs and control medium on MDA-MB-231 cells by MTT assay after incubation with different concentrations of stock solution for 24 hrs. These experiments are performed in triplicate and represented as the mean ± SD.

3.3.8 Cell Imaging

The excellent biocompatibility (no cytotoxicity), high quantum yield, excellent photostability, and wide range pH. sustainability of the prepared FMNCs made it possible to examine their property for cell imaging. This was pursued by incubating HaCaT cells with FMNCs ($1/10^{th}$ of 30 mg/ml stock) for 24 hrs in DMEM. After removing the medium, the cells were washed with PBS (pH-7.4) to remove unbounded FMNCs and, afterward, observed under a confocal microscope and found that the FMNCs exhibit fluorescence in both green and red channels, which demonstrates significant cytoplasmic accumulation of FMNCs (Figure. 3.10 a, b). The corresponding merged and bright field images are shown in (Figure. 3.10 c, d).

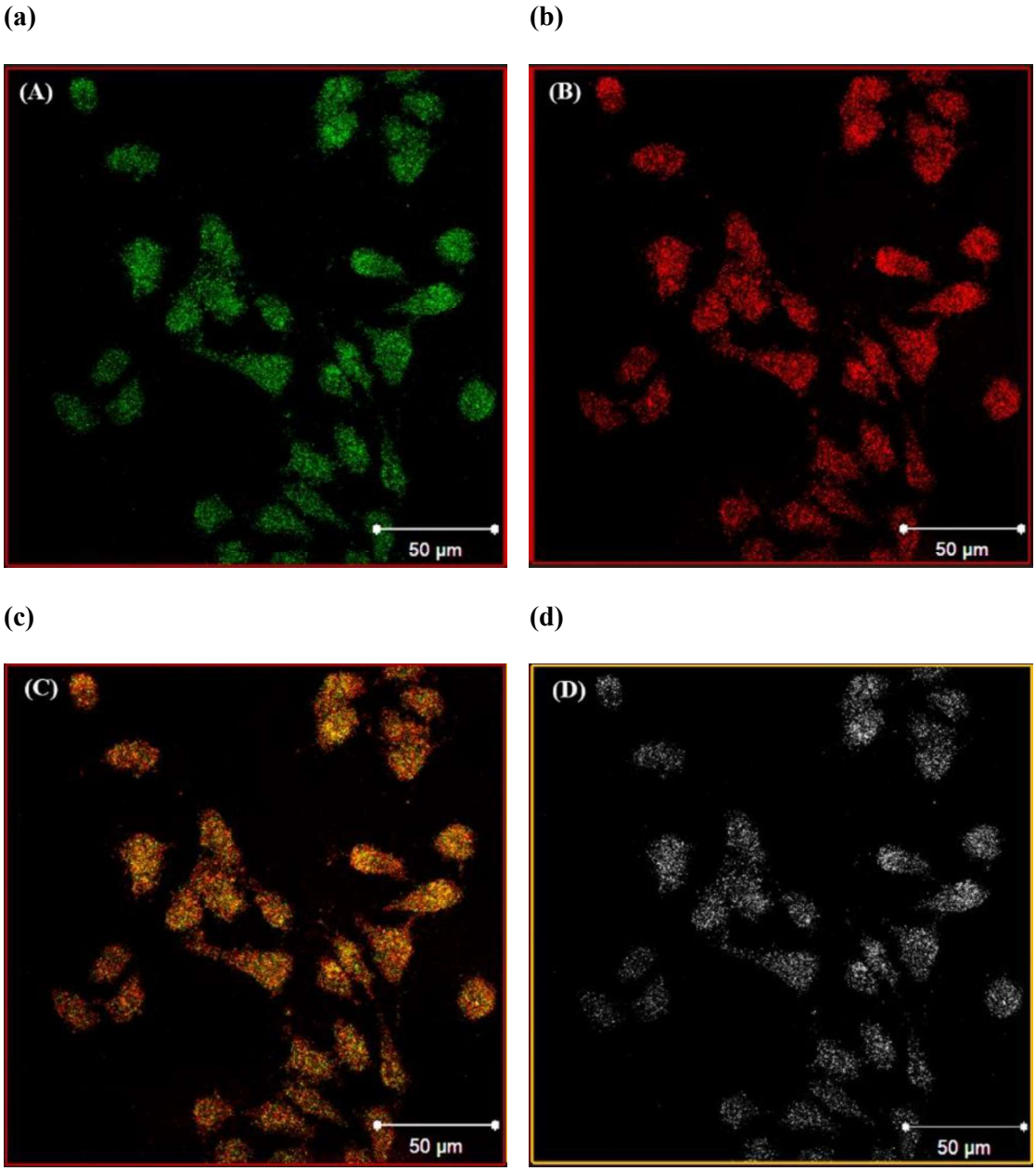

Figure. 3.10 Multi fluorescent image of HaCaT cells incubated with FMNCs ($1/10^{th}$ of stock solution) (A) Ex. 472 nm / Em. Green (B) Ex. 472 nm / Em. Red (C) merged image (D) Bright-field image.

3.4 Conclusion

In conclusion, we successfully synthesized 1.6 ± 0.6 nm big, highly biocompatible and water soluble Mg^0 nanoclusters using BSA and ascorbic acid. These nanoclusters showed excitation-dependent emission and broad-spectrum white light emission (CIE (0.3, 0.33)) under UV excitation. Furthermore, synthesized nanoclusters luminesced in blue, green, and red regions with an average lifetime of 2.94, 3.07, and 0.3 ns. The MALDI-TOF results clearly show that these nanoclusters are 28, 609, and 1396 atoms big. Further studies showed 100 % cell viability of HEK-293 cells when incubated with 0.3,0.03 mg/ml FMNCs. The FMNCs (Mg^0 nanocluster) were successfully used as a fluorescent label to image HaCaT cells using a confocal microscope with red, green, and orange channels. Further, developed Mg^0 nanoclusters show significant fluorescence (with 20-30% loss) emission intensity even after 8 months of storage. Current work envisions the applicability of these fluorescent and biocompatible FMNCs in nanomedicine and various other areas of energy and display.